Hydrodynamics of microplasmas from thin foils exploded by picosecond laser pulses *

Paola Squillacioti, Marco Galimberti, Luca Labate,† Paolo Tomassini, and Antonio Giulietti
Intense Laser Irradiation Laboratory - IPCF, Area della Ricerca CNR, Via Moruzzi 1, 56124 Pisa, Italy

Valery Shibkov
Dep. of Physics, Moskow Sate University, Moskov, Russia

Flavio Zamponi
IOQ, Fredrich-Schiller University, Jena, Germany
(Dated:)

Thin plastic foils have been exploded by 30 picosecond laser pulses at an intensity ranging from 10^{14} $\frac{W}{cm^2}$ to 10^{15} $\frac{W}{cm^2}$. The hydrodynamic evolution of the plasma has been studied by interferometry for two different foil thicknesses, 300 and 900 nm respectively. The plasma produced beyond the foil shows sistematically a different dynamics in the two cases. In the case of 300 nm foil, such a dynamics appears to be driven by the radiation pressure of the laser pulse. This explanation is supported by 2D simulation.

PACS numbers: 52.50.Jm, 52.25.Jm, 52.25.Os, 52.38.Bv, 42.87.Bg.

I. INTRODUCTION

Intense Laser irradiation and consequent explosion of thin foils is an established method to produce laboratory plasmas. The method has been originally introduced to produce linear plasmas, suitable for x-ray plasma lasing experiment [1]. Preformed plasmas from foils exploded by nanosecond pulses have been also extensively used for laser-plasma interaction experiments, mostly devoted to the study of instabilities affecting the energy transfer in direct-drive Inertial Confinent Fusion experiments [2] [3] [4]. This kind of microplasmas produced with nanosecond laser pulses have been carefully characterised in density and temperature at different delays from their formation [5] [6]. The plasma parameters were found to depend on laser intensity and wavelength, pulse duration, foil thickness and material, as expected from analytical models [7] and numerical codes [8], [9], [10], [11] that describe the hydrodynamic expansion of such plasmas. A characteristic time in the process is the burn-through time at which, due to the expansion, most of the laser light goes through the underdense plasma. Whether the laser pulse duration is larger or smaller than the burn-through time, is a discriminant in the level of laser energy deposition in the plasma, and in the possibility of direct laser energy transfer beyond the foil target. More generally, with nanosecond pulses at moderate intensity, after the end of the laser pulse, the plasma density evolves hydrodynamically with a simmetry around the normal to the foil, irrespectively of the direction of the heating laser beam. In this work we show that this is not the case with picosecond intense pulses heating thin targets.

II. EXPERIMENTAL SETUP

The laser system we used delivers light pulses of 1064 nm wavelength and duration 30 ps Full Width Half Maximum (FWHM). The laser beam was divided in two parts by a beam-splitter. The major part (main pulse) was sent into the vacuum chamber and focused by a $f/8$ lens in a 12 μm diameter spot (which provided an intensity up to 10^{15} W/cm^2). The focused beam is p-polarized and reached the foil at an angle of 20° with respect to the foil normal. The laser pulse energy and the quality of the focal spot were monitored, shot by shot, by using an equivalent plane technique. The target was a stripe of 0.5 mm width of plastic material (Formvar); we used two foil thicknesses: 300 and 900 nm.
A minor portion of the beam was frequency-doubled, filtered from residual components of infrared light and used as probe pulse through the plasma in a Nomarsky interferometer [12]. The probe was parallel to the foil and perpendicular to the laser beam axis.
The basic element of this interferometer is the Wollaston prism that produces two separate orthogonally polarized images of the plasma surrounded by an unperturbed background. Interference between each of the two images and the background of the other image is achieved by a polarizer oriented at 45° with respect to the two polarization axes. The resulting interferometric pattern was acquired with a Charge Coupled Device (CCD) camera. The delay of the probe beam with respect to the main pulse was varied by moving a prism mounted on an optical guide.
Laser-plasma interferograms were analyzed by extracting the phase-shift map with a technique based on Continuous Wavelet Transforms (Interferogram Analysis by Continuos wavelet transform Ridge Extraction, IACRE),

*This work is dedicated to the memory of G.P. Banfi, a pioneer in the field of laser-plasma interactions.
†Also at Dipartimento di Fisica Università di Bologna, Bologna, Italy

which was proved to be more effective than the usual Fast Fourier Transform (FFT) based methods [13][14]. Then we used a generalized [15] Abel inversion algorithm, where the axial symmetry is partially relaxed, to obtain the density map.

The interferograms are characterized by the fringe visibility and the resolution. The resolution depends on the minimum fringe shift that the analysis program can resolve. As we had a good visibility, the program could resolve $\frac{1}{10}$ of fringe which corresponds to 1.8 μm. The good visibility we had at probing times much longer than the pulse duration is due to the use of a short probe pulse compared with time scale of density changes and the use of the second harmonic which increases the probe pulse contrast. Using the second harmonic we could also put an interferential filter to avoid the diffusion of the fundamental frequency in the interferograms. Moreover, the shorter wavelength allows a decrease of the probe ray bending, an effect which is responsible for the anomalous fringe distortion and the reduction of the fringe visibility.

III. INTERFEROGRAMS

In figure 1 we can see four patterns representative of a large number of interferograms obtained during the experiment. They were obtained at different probe delays with respect to the main pulse. The interferograms of the left column refer to 900 nm foils, the others to 300 nm foils. In all these cases the delays were much longer than the pulse duration, so that they give us infomation about the plasma evolution at long time. For each interferogram two white arrows indicate respectively the normal to the foil and the direction of the laser propagation. The intersection point of the two arrows indicates, with a good approximation, the focus of the laser. It lies, generally, inside the vertical black stripe that is the foil shadow on the interferogram. The bigger dimension of the shadow in the focal region, with respect to the unperturbed target shadow, is due to the target expansion in the marginal (cold) region of the interaction. This doesn't mean necessarily that in that zone there is a overdense plasma. This area of shadow defines the spatial limit of the fringe visibility (i.e. of the electron density measurement).

From the interferograms it's clear that, at the times considered, a plasma also exists beyond the target. Estimations done with an analytical self-similar model [7] and results more precise obtained with an hydrodynamic code 2D (POLLUX) [10] clearly show that, during the pulse, the laser energy can't be transferred directly beyond the foil. In fact, to have a transfer of the laser energy, we must have the burn through condition for the laser radiation: the plasma must be completely underdense before the end of the pulse. In our case the critical density is $n_c = 1.1 \cdot 10^{21}\ cm^{-3}$. The simulation says that at an intensity of $10^{15}\ \frac{W}{cm^2}$, that is the upper limit of the intensities used, the burn through time is 100 ps for a 300 nm foil and bigger for a 900 nm foil. This means that for the whole pulse duration (30 ps FWHM) there isn't laser energy deposition beyond the foil. Then the plasma formation beyond the foil must be attribuited to indirect transport mechanisms, and basically to the electron conduction by the plasma electrons. The hydrodynamic code predicts at the peak of the pulse a maximum in electron temperature of 3 KeV, located at the critical density layer. It's clear that denser plasma regions of the foil are heated by conduction (and by absorption of more penetrating radiation emitted by the plasma) beyond the critical layer. This heating process continues also after the end of the laser pulse and this mechanism is responsible of the plasma creation beyond the foil. The interferograms show that this plasma has a different geometry from the plasma that expands from the front part of the foil: it appears less developed transversally. This probably indicates a collimation of part of the electrons that transport energy, in particular the hotter and faster electrons. The collimation can be due to a self-generated magnetic field.

A typical, experimental electron density distribution of the plasma in front and beyond the foil is shown in Fig.2, as derived from the fringes system of the Fig.1.b. That distribution was obtained from the interferograms with the methods of numerical analysis and deconvolution indicated previously. The deconvolution was possible from -30 μm with respect to the target position towards the laser and from 20 μm in the opposite direction. The distribution of the electron density obtained from the other interferograms are not shown here. The comparison of those distributions with the electron density expected by the 2D code shows that numerical results underestimate the electron density at distances greater than 30 μm from the foil and overestimate the scale length in the same region.

It's particularly interesting the comparison between the fringe patterns obtained from the 900 nm foil and the ones from the 300 nm foil. In fact, while in the former case the plasma beyond the foil expands around a simmetry axis roughly corresponding to the normal to the foil, in the latter case the plasma beyond the foil expands around an inclined axis, close to the direction of the laser propagation. This behaviour is common to all the interferograms obtained with 300 nm foils.

Further, in one case (Fig.3) also the ejection of a "plasma particle" was observed at an angle with respect to the normal. It's a pellet of ionized material, whose physical parameters could be evaluated by the interferometric analysis conducted with the IACRE method. First of all, we found that this pellet contains $N_e \approx 3 \cdot 10^{12}$ free electrons. If we suppose that the pellet is completely ionized, we can attribute to it a mass of $m \approx 2 \cdot 10^{-12}\ g$; since we cannot exclude a partial ionization, this is a lower limit to the real mass. This mass is located at 218 μm from the foil after 1.1 ns. If we assume that the pellet was ejected during the laser pulse, its ejection velocity is $v \approx 2 \cdot 10^7\ \frac{cm}{s}$. The data relative to the plasma pellet is

summarised in the table below, where E_c is the kinetic energy and E_L the energy of the laser pulse.

IV. DISCUSSION

The interesting observations relative to the plasma dynamics beyond the 300 nm foil (consequent to an expansion not perpendicular to the foil) were not reproduced in the 900 nm case. To interpret this behaviour of the plasma we have excluded the laser propagation beyond the foil, since the burn through time is bigger than the pulse duration also in the case of 300 nm foil. Also, effects due to shock waves don't seem applicable in a direction different from the foil normal. We can consider the action of fast suprathermal electrons created during the laser-foil and laser-plasma interactions. The production of fast electrons (definitely more energetic than thermal electrons) is very likely in our experiment, where the resonant absorption is expected to play a major role. In fact the simulation points out that around the critical density there is a gradient with a scale length, during the pulse, of the order of 1 μm. In this condition the laser radiation polarized "p" that arrives with an angle of 20° has a high coefficient of resonant absorption. In fact [16] [17] the expression of the coefficient of resonant absorption f_R is:

$$f_R \simeq \frac{1}{2.8}\phi^2(q) \simeq 18q\frac{A(q)^3}{|\dot{A}|} \qquad (1)$$

where ϕ is Denisov's function; A, $\dot{A}$ are the Airy function and its derivative; $q = (k_0 L)^{\frac{2}{3}} sin^2\theta$ and k_0 the vacuum wavenumber of the radiation. The coefficient of resonant absorption f_R is a rather smooth function of q having its maximum value $f_R^{Max} \simeq 0.5$ approximately at $q = 0.4$. If we consider our values: $k_o \sim 2\pi\ \mu m^{-1}$, $L \sim 1\ \mu m$ and $\theta = 20°$, we obtain $q = 0.4$ which corresponds to the maximum of f_R.

This electromagnetic energy deposition close to the critical layer favors the growth of longitudinal electronic waves of big amplitude that contribute to the electron acceleration at energies bigger than the thermal energies. However, at the intensities and with the duration of the pulse used in our experiment we can exclude the acceleration of collimated electron beams in the laser direction, as has been observed with femtosecond pulse at relativistic intensities [18] [19] [20]. Then, though we can attribute a relevant role to the fast electrons, we cannot attribute directly to them the anomalous expansion of the plasma we have observed beyond the 300 nm foils.

We think that the most probable mechanism to which attribute the effect we have observed is the radiation pressure exerted by the laser pulse on the plasma. This force, in the case in which the absorption prevails over the reflection (that seems to be our case), is directed along the pulse propagation direction. In general such a radiation force will be exerted at an intermediate direction between the foil normal (case of pure reflection) and the laser direction (case of total absorption). In fact, in the case where this direction is easier to evaluate (Fig.3), the angle of ejection of the pellet with respect to the foil normal is $\sim 15°$.

At the intensity of $I = 1 \cdot 10^{15}\ \frac{W}{cm^2}$ and in the case of total absorption, the pressure radiation at the peak pulse can be estimated as

$$P_r = \frac{I}{c} \approx 3{\cdot}10^{10}\frac{N}{m^2}, \text{ i.e. about } 3{\cdot}10^5 \text{ Atmosphere.} \qquad (2)$$

We can have an idea of the possible action of such a pressure: if it would be applied to a pellet of 10^{-12} grams with a surface comparable to the focal spot for a time of 10 ps, the pellet could be accelerated to a velocity of $2 \cdot 10^7\ \frac{cm}{s}$. Why this pressure can drive a plasma expansion beyond the foil in the case of 300 nm foil and not in the case of 900 nm? The diagrams of Fig.4 help us to answer this question. These diagrams were obtained with the 2D hydrodynamic code POLLUX. They report the temperature, the matter density and the electron density at the peak of the laser pulse for 300 and 900 nm foils, respectively. As expected, the profiles in front of the foil (toward the laser) cannot be distinguished in the two cases. The critical layer is localized at about 1.8 μm from the original position of the irradiated surface. In this region we can observe a clear profile-steepening, according to a strong resonant absorption and a peak temperature of about 3 KeV. Instead the profiles are different inside the foil (the shaded zones are the regions originally occupied by the target). In this region the POLLUX code cannot provide a reliable value for the electron density, but we can infer it from temperature and matter density. In both cases the peak of the matter density shifts away from the laser with respect to the original target position because of the reaction to the ablation produced by the first part of the pulse. In the case of 900 nm foil the major part of the dense region is very cold, still solid and not ionized. It can resist the pressure radiation. The plasma beyond the foil will form after the end of the laser pulse. Instead, in the case of 300 nm foil all the dense region has a temperature higher than 10 eV, and is then strongly ionized. Basically in this case we have a plasma which cannot resist to the action of the radiation pressure exerted by the laser on the critical layer and transferred to the overcritical region a few μm's behind.

Concerning the "plasma particle" observation described before, plasma " bullets" accelerated toward the laser have been observed recently also in an experiment of 100 ps laser pulse irradiation on massive Al targets in air [22]. In the condition of that experiment, the bullets originate from the critical layer of the shock wave propagating in air. The condition of our experiment are quite different. However, the interpretative model supplied in [22] can be in principle considered also in our case. Such a model is based on the generation (experimentally proved in that experiment) of a magnetic fields able to accelerate plasma particles. Though the model of [22] seems

not to explain all our observations, the contribution of a self generated magnetic field cannot be excluded in the acceleration of plasma particles also in our case.

In conclusion we have found, to our knowledge for the first time, that some energy can be transferred beyond an overdense plasma in a direction roughly coincident with the propagation of the laser beam. This process is likely to be driven by the laser radiation pressure. In this way also plasma pellets can be accelerated to very high velocity.

Acknowledgments

The authors acknoweledge D.Giulietti and L.A.Gizzi for many helpful discussions and Antonella Rossi for the careful target preparation.

The work has been partially supported by Consiglio Nazionale delle Ricerche, Italy. The collaboration of one of the authors was granted by Ministero degli Esteri of the Italian Government in the framework of the Italia-Russia agreement. Some authors (M.G., L.L and P.T) wish to acknowledge support from italian M.I.U.R. through the Project 'Metodologie e diagnostiche per materiali e Ambiente'.

[1] D.L. Matthews, P.L.Hagelstein, M.D.Rosen *et al.*, Phys. Rev. Lett. **54**, 110 (1985).
[2] R.E. Turner, Kent Estabrook, R.L.Kauffman, D.R.Bach, R.P.Drake, D.W.Phillion, B.F.Lasinski, E.M.Campbell, W.L.Kruer, and E.A.Williams, Phys. Rev. Lett. **54**, 189 (1985).
[3] A. Giulietti, D.Giulietti, D.Batani, V.Biancalana, L.Gizzi, L.Nocera, and E.Schifano, Phys. Rev. Lett. **63**, 524 (1989).
[4] T. Afshar-Rad, L.A.Gizzi, M.Desselberger, F.Khattak, and O.Willi, Phys. Rev. Lett. **68**, 942 (1992).
[5] L.A.Gizzi, D.Giulietti, A.Giulietti, T.Afshar-Rad, V.Biancalana, P.Chessa, E.Schifano, S.M.Viana, and O.Willi, Phis. Rev. E **49**, 5628 (1994).
[6] M.Borghesi, A.Giulietti, D.Giulietti, L.A.Gizzi, A.Macchi, and O.Willy, Phis. Rev. E **54**, 6769 (1996).
[7] Richard A.London and M.D.Rosen, Phys. Fluids **29**, 11 (1986).
[8] J.P.Christiansen, D.E.T.F.Ashby, and K.V.Roberts, Comput. Phys. Commun. **7**, 271 (1974).
[9] A.Djaoui and S.J.Rose, J. Phys. B: At. Mol. Opt. Phys. **25**, 2745 (1992).
[10] G.J.Pert, J. Comp. Phys. **43**, 111 (1981).
[11] L.Labate, M.Galimberti, A.Giulietti, D.Giulietti, L.A.Gizzi, and R.Numico, Laser and Particle Beams **20**, 223 (2002).
[12] R.Benattar, C.Popovics, and R.Sigel, Rev. Sci. Instrum. **50**, 12 (1979).
[13] P.Tomassini, A.Giulietti, L.A.Gizzi, M.Galimberti, D.Giulietti, M.Borghesi, and O.Willi, Appl. Optics. **40**, 6561 (2001).
[14] P.Tomassini, A. Giulietti, L.A. Gizzi, R.Numico, M.Galimberti, D.Giulietti, and M.Borghesi, Laser and Particle Beams **20** 2 195-199 (2002).
[15] P.Tomassini and A.Giulietti, Optics Comm. **199**, 143 (2001).
[16] T.P.Hughes, Proceedings of the Twentieth Scottish Universities Summer School in Physics St. Andrews, August 1979, edited by R.A.Cairns and J.J.Sanderson, p.1.
[17] G.P.Banfi, P.G.Gobbi, S.Morosi, and G.C.Reali, Appl. Phys. Lett. **37**, 23 (1980).
[18] T.Tajima and J.M.Dawson, Phys. Rev. Lett. **43**, 267 (1979).
[19] C.Gahn, G.Tsakiris, A.Pukov, J.Meyer ter Vehn, G.Pretzler, P.Thirolf, D.Habs, and K.J.Witte Phys. Rev. Lett. **83**, 4772 (1999).
[20] D.Giulietti, M.Galimberti, and A.Giulietti *et al.*, Phys. Plasmas **9**, 9 (2002).
[21] P.Mulser, Proceedings of the Twentieth Scottish Universities Summer School in Physics St. Andrews, August 1979, edited by R.A.Cairns and J.J.Sanderson, p.91.
[22] Nadja I. Vogel and N.Kochan, Phys.Rev.Lett. **86**(2), 232 (2001).

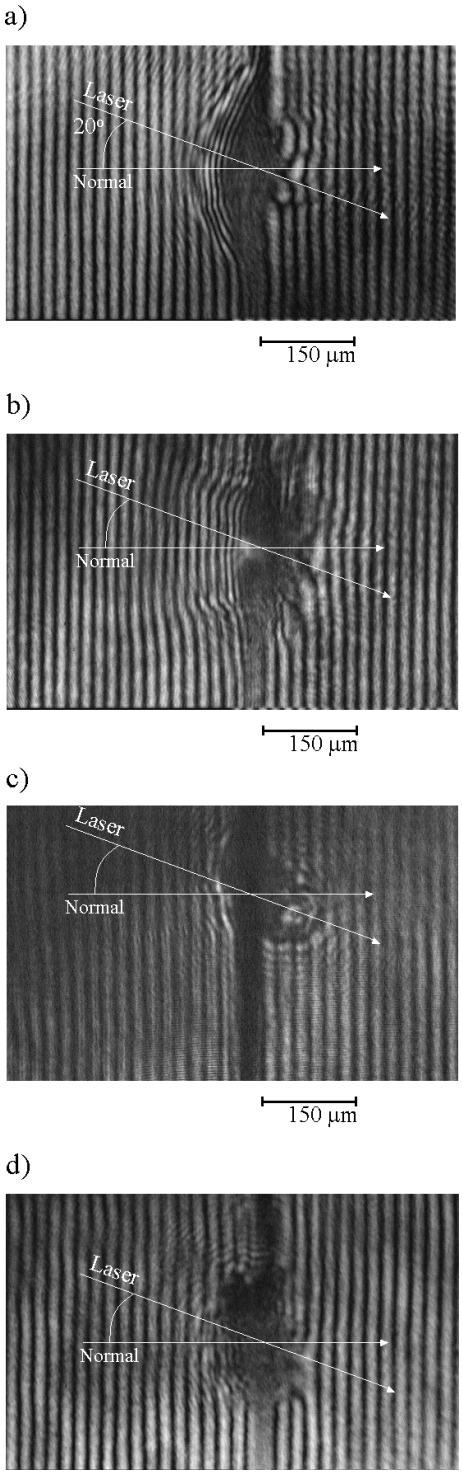

FIG. 1: Interferograms: foil thickness: a),b) 900nm; c),d) 300nm; intensity on target: a) $6.4 \cdot 10^{14}$ $\frac{W}{cm^2}$; b) $6.3 \cdot 10^{14}$ $\frac{W}{cm^2}$; c) $2.3 \cdot 10^{14}$ $\frac{W}{cm^2}$; d) $5.3 \cdot 10^{14}$ $\frac{W}{cm^2}$; probe delay: a) 0.6 ns; b) 1.4 ns; c) 0.9 ns; d) 1.1 ns.

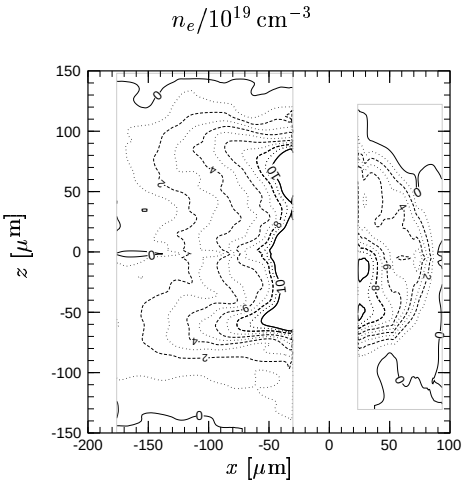

FIG. 2: Electron density map from the interferogram b) of figure 1.

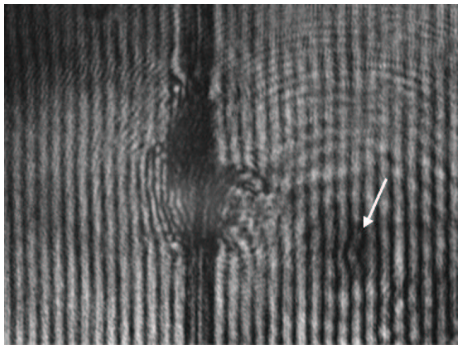

FIG. 3: Interferogram obtained with 300 nm thick Formvar. I = $3.2 \cdot 10^{14}$ $\frac{W}{cm^2}$. The probe delay is 1.1 ns. The arrow indicates the position of the expelled ionized foil fragment.

TABLE I: Physical parameters of the plasma pellet evidenced by the interferograms of Fig.3

N_e	$\simeq 2 \cdot 10^{12}$ free electrons
m	$\sim 2 \cdot 10^{-12}$ g
v	$2 \cdot 10^{7}$ $\frac{cm}{s}$
E_c	$\simeq 30$ μj
$\frac{E_c}{E_L}$	$\approx 10^{-3}$

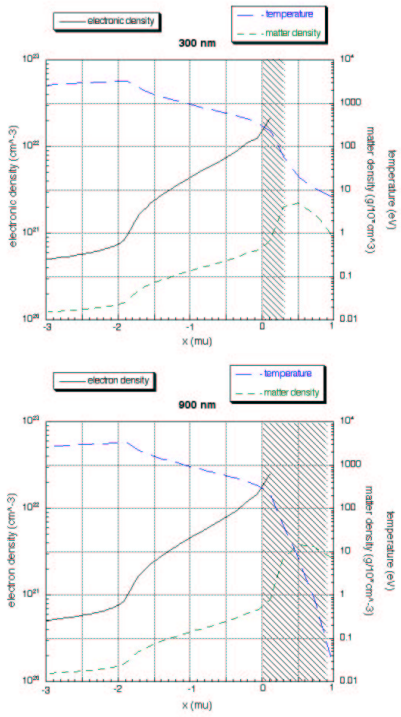

FIG. 4: Mass density, electron density and temperature profiles at the peak of the laser pulse. Laser Intensity: $2 \cdot 10^{14} \frac{W}{cm^2}$.